

New Dispiro Compounds: Synthesis and Properties

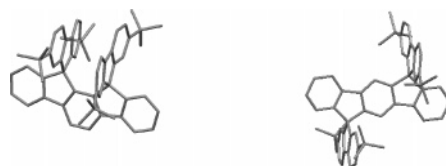
Cyril Poriel,^{*,†,‡} Joëlle Rault-Berthelot,^{*,†,‡} Frédéric Barrière,^{†,‡} and Alexandra M. Z. Slawin[§]

Université de Rennes 1 and CNRS UMR 6226 “Sciences Chimiques de Rennes” Equipe ‘Matière Condensée et Systèmes Electroactifs’ (MaCSE) Bat 10C, Campus de Beaulieu, 35042 Rennes cedex, France, and School of Chemistry, University of St. Andrews, Fife, Scotland KY16 9ST, U.K.

cyril.poriel@univ-rennes1.fr; joelle.rault-berthelot@univ-rennes1.fr

Received October 29, 2007

ABSTRACT



We report the synthesis and structural characterization of two dispiro compounds. These two positional isomers have been designed and synthesized through an efficient method. Because of the rigidity and orthogonality of the spiro bridge, both molecules exhibit a well-defined architecture which consists of two fluorene rings connecting to an indenofluorenyl unit via two sp^3 carbon atoms. The structural, electrochemical, optical, and thermal properties of these dispiro isomers are discussed.

Organic molecules/polymers with a π aromatic backbone are capable of transporting charge, and thus, these systems may behave as semiconductors in opto-electronic devices.¹ In addition, organic chemistry offers a versatile means of tailoring the properties of molecules/polymers, which is not possible for traditional inorganic materials. Compared to extended π conjugated polymers, small molecular units with well-defined conjugation lengths are characterized by the absence of chain defects, are easier to purify, and are prone to full characterization.^{2,3} This makes these molecules more attractive than extended π -conjugated polymers for investigations of the structure–property relationships.⁴ In this context, several families of molecular architectures have been

developed and exploited, such as twin molecules, orthogonally fused spiro-type molecules, paracyclophane, dendrimers, or C_3 symmetry starburst molecules.⁴ In our quest for efficient materials for blue organic light emitting diodes (OLED), we recently designed a new family of luminescent dispiro derivatives, dispiro[fluorene-9,6'-indeno[1,2-*b*]fluorene-12',9''-fluorene] called **(1,2-*b*)-DSF-IFs**.^{5,6} As recently reported by different groups, such dispiro structures appear to be highly promising for blue OLED application.^{7–11} On the other hand, (1,2-*b*)-indenofluorene (**(1,2-*b*)-IF**) has been

[†] Université de Rennes 1.

[‡] CNRS UMR 6226.

[§] University of St. Andrews.

(1) Müllen, K.; Scherf, U. *Organic Light-Emitting Devices: Synthesis, Properties and Applications*; Wiley-VCH Verlag GmbH & Co. KGaA: Weinheim, 2006.

(2) Tour, J. M.; Wu, R.; Schumm, J. S. *J. Am. Chem. Soc.* **1990**, *112*, 5662–5663.

(3) Wu, R.; Schumm, J. S.; Pearson, D. L.; Tour, J. M. *J. Org. Chem.* **1996**, *61*, 6906–6921.

(4) Cao, X.-Y.; Zhang, W.; Pei, J. *Org. Lett.* **2004**, *6*, 4845–4848 and references therein.

(5) Horhant, D.; Liang, J.-J.; Virboul, M.; Poriel, C.; Alcaraz, G.; Rault-Berthelot, J. *Org. Lett.* **2006**, *8*, 257–260.

(6) Poriel, C.; Liang, J.-J.; Rault-Berthelot, J.; Barrière, F.; Cocherel, N.; Slawin, A. M. Z.; Horhant, D.; Virboul, M.; Alcaraz, G.; Audebrand, N.; Vignau, L.; Huby, N.; Hirsch, L.; Wantz, G. *Chem. Eur. J.* **2007**, *13*, 10055–10069.

(7) Kimura, M.; Kuwano, S.; Sawaki, Y.; Fujikawa, H.; Noda, K.; Taga, Y.; Takagi, K. *J. Mater. Chem.* **2005**, *15*, 2393–2398.

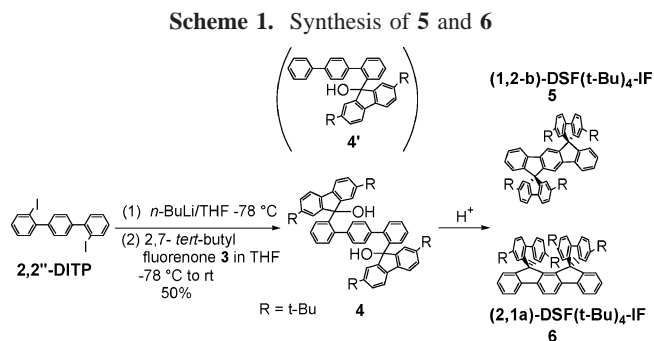
(8) Xie, L. H.; Hou, X.-Y.; Tang, C.; Hua, Y.-R.; Wang, R.-J.; Chen, R.-F.; Fan, Q.-L.; Wang, L.-H.; Wei, W.; Peng, B.; Huang, W. *Org. Lett.* **2006**, *8*, 1363–1366.

(9) Vak, D.; Lim, B.; Lee, S.-H.; Kim, D.-Y. *Org. Lett.* **2005**, *7*, 4229–4232.

(10) Harrington, L. E.; Britten, J. F.; Mc Glinchey, M. J. *Org. Lett.* **2004**, *6*, 787–790.

(11) Wu, Y.; Zhang, J.; Bo, Z. *Org. Lett.* **2007**, *9*, 4435–4438.

widely used for the last 10 years as a central building block within the backbone of polymers or oligomers leading to a strong enhancement of the OLED properties.^{9,12–14} However, to the best of our knowledge, the **(2,1-*a*)-IF** positional isomer has only been reported in two instances^{15,16} and is unknown with spiro linkages. In this context, we thus designed and prepared, through an expedient synthesis, two new dispiro chromophores, **(1,2-*b*)-DSF(*t*-Bu)₄-IF 5** and **(2,1-*a*)-DSF(*t*-Bu)₄-IF 6**, with shape persistent molecular architectures and different geometric profiles, i.e., linear antarafacial and suprafacial geometries.⁸ The synthetic route is presented in Scheme 1. It is based on a coupling reaction between



diiodinated terphenyl (**2,2''-DITP**)⁶ and 2,7-*tert*-butylfluorenone **3**, followed by a key intramolecular cyclization reaction. From a statistical point of view, this cyclization step may occur on either side of the terphenyl backbone and should lead to the **(1,2-*b*)-DSF(*t*-Bu)₄-IF 5** and **(2,1-*a*)-DSF(*t*-Bu)₄-IF 6**. Although the bulkiness of the *tert*-butyl substituents should in principle favor the less sterically hindered positional isomer we expected the formation of both isomers. Indeed, the formation of conceptually related positional isomers from a terphenyl backbone has been previously observed with indolocarbazole derivatives by Leclerc and co-workers.^{17,18} Theoretical calculations (full optimization on simplified models of the two isomers without *tert*-butyl groups at the B3LYP/6-31G* level of theory vide infra) indicate that the **5**-like isomer is only less than 8 kcal mol⁻¹ more stable than the **6**-like isomer.

As shown in Scheme 1, the lithium–iodine exchange of **2,2''-DITP** with *n*-butyllithium at low temperature followed by quenching with 2,7-*tert*-butylfluorenone **3**^{19,20} afforded

the difluoreneol **4** in moderate yield (50%). This reaction appeared to be highly sensitive to the dilithiate intermediary formation time. Indeed, a byproduct, identified as the monoalcohol **4'** by X-ray crystallography is always formed (cf. the Supporting Information). Very short reaction time for metal–halogen exchange followed by immediate quenching with **3** is essential to minimize the formation of **4'**. The intramolecular cyclization reaction performed in acidic medium leads to the expected formation of **5** and **6**. These molecules possess two spiro-linked fluorene rings and a central **IF** backbone (1,2-*b*- or 2,1-*a*-substituted). Compound **6** appears to be the first example of a spiro-linked **(2,1-*a*)-IF** core. As shown in Table 1, the conversion of the diol **4**

Table 1. **6/5** Ratio for Different Reaction Conditions

solvent	<i>T</i> (°C)	6/5 ratio ^a (%)	reaction time (min)	acid
CH ₂ Cl ₂	0	19/81	30	H ₂ SO ₄
CH ₂ Cl ₂	rt	24/76	30	H ₂ SO ₄
AcOH	5 to rt ^b	40/60	overnight	HCl
AcOH	rt to 70	50/50	180	HCl
AcOH	reflux	60/40	120	HCl

^a The **6/5** ratio was determined from the ¹H NMR spectrum of the crude reaction before any treatment. ^b 3 h at 5 °C and overnight at rt.

to **5** and **6** is highly sensitive to the reaction conditions, including the acid, the solvent, and the reaction temperature. Preliminary studies indicate that the ratio of these two isomers may be strongly modulated going to a **6/5** ratio of 19/81 to 60/40 depending on these reaction conditions. The isolated yields of both isomers are in each case greater than 80%.

The two isomers **5** and **6** were easily separated by column chromatography. Heteronuclear multiple bond correlation (HMBC) spectra were performed for both isomers in order to ascertain their molecular structures through long-range shift correlations. In this context, the spiro carbons are powerful probes to detect neighboring hydrogens. For **5**, three cross-peaks are observed for the spiro carbon atoms corresponding to three-bond correlations (³*J*) with H_a (7.21 ppm), H_b (6.74 ppm), and H_c (6.65 ppm), Figure 1a. The spectrum of **6** exhibits only two ³*J* correlations with the spiro carbon

(12) Grimsdale, A. C.; Müllen, K. *Macromol. Rapid. Commun.* **2007**, *28*, 1676–1702.

(13) Jacob, J.; Zhang, J.; Grimsdale, A. C.; Müllen, K.; Gaal, M.; List, E. J. W. *Macromolecules* **2003**, *36*, 8240–8245.

(14) Merlet, S.; Birau, M.; Wang, Z. Y. *Org. Lett.* **2002**, *4*, 2157–2159.

(15) Deuschel, W. *Helv. Chim. Acta* **1951**, *34*, 2403–2416.

(16) Covion Organic Semiconductors; Eur. Pat. Appl., EP 1491568, 2004.

(17) Blouin, N.; Michaud, A.; Wakim, S.; Boudreault, P.-L. T.; Leclerc, M.; Vercelli, B.; Zecchin, S.; Zotti, G. *Macromol. Chem. Phys.* **2006**, *207*, 166–174.

(18) Wakim, S.; Leclerc, M. *Synlett* **2005**, *8*, 1223–1234.

(19) Weber, E.; Dörpinghaus, N.; Csöreg, I. *J. Chem. Soc., Perkin Trans. 2* **1990**, 2167–2177.

(20) Stigers, K. D.; Koutroulis, M. R.; Chung, D. M.; Nowick, J. S. *J. Org. Chem.* **2000**, *65*, 3858–3860.

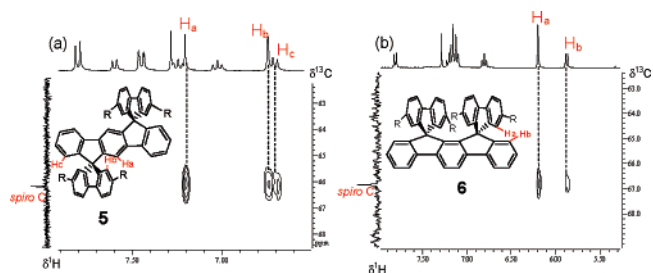


Figure 1. Portion of the HMBC (CDCl₃) spectra of (a) **5** and (b) **6**.

atoms assigned to H_a (6.20 ppm) and H_b (5.87 ppm), Figure 1b. The absence of a third correlation is consistent with the long distance separating the hydrogen atoms of the **(2,1-a)-IF** central phenyl ring and the spiro carbon atoms.

Single crystals of **5** and **6** obtained by slow diffusion of hexane into a CDCl₃ solution were analyzed by X-ray diffraction in order to study their detailed molecular structure (Figure 2). In these two structures, the fluorene rings adopt

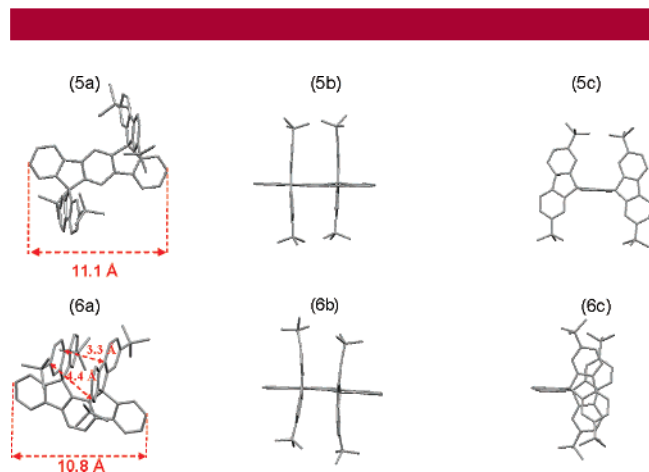


Figure 2. Molecular structure of **5** and **6**. Top (a) and side views (b and c), from single-crystal X-ray data.

a “saddle shape” twist (cf. the Supporting Information for definitions and calculations of the folding angles of the fluorene rings). In **5**, the fluorene rings are folded, with two minor distortions on each side, caused by the two *tert*-butyl substituents, that stretch inside of the rigid H shape (Figure 2, view 5b). In **6**, the folding of the fluorene rings is more pronounced. Contrary to the isomer **5** and in order to avoid any strong steric interactions, the fluorene rings are stretched outside of the H shape (Figure 2, view 6b). The distance between the two opposite carbon atoms bearing *tert*-butyl substituents is ca. 4.4 Å. The shortest distance between opposite carbon atoms is 3.3 Å (Figure 2, view 6a), which is smaller than the sum of the van der Waals radii. It should also be noted that, for both structures, the spiro carbons are not perfectly in the plane of the indenofluorenyl moieties (cf. the Supporting Information). Indeed, in the solid-state structure of **6**, a slight tilt is observed for the two spiro carbons, one pointing above the indenofluorenyl plane (through the central phenyl ring) and the other pointing below this plane (Figure 2, view 6c). This up/down structural feature is assigned to the spiro linkage of the **(2,1-a)-IF** core. In the case of **5**, the spiro carbons are both pointing on the same side of the indenofluorenyl plane.

The electrochemical properties of **5** and **6** were investigated by cyclic voltammetry (CV) and compared with the nonsubstituted **(1,2-b)-DSF-IF** and with the two molecular building blocks of **5**, i.e., **(1,2-b)-IF** and 2,7-*tert*-butyl fluorene **2** (Figure 3, Table 2). The first oxidation of **(1,2-b)-IF** is monoelectronic and reversible and occurs at 1.31 V. A similar oxidation process occurs at 1.33 V for **5**. On the other hand, the CV of **2** exhibits a first reversible

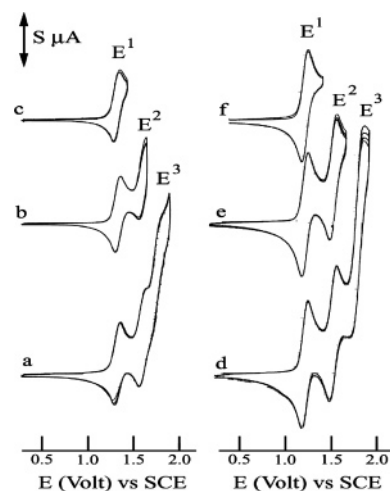


Figure 3. Anodic oxidation of a 1.35 10⁻³ M solution of **5** (a–c) and 1.30 × 10⁻³ M of **6** (d–f) in CH₂Cl₂ + Bu₄NPF₆ 0.2 M. Sweep rate: 100 mV/s. S = 4 μA. Pt disk working electrode (diameter 1 mm).

oxidation wave at 1.44 V (cf. the Supporting Information). In the cathodic range (data not shown), the reversible monoelectronic reduction occur at –2.36 and –2.52 V for

Table 2. Electrochemical Properties and HOMO/LUMO Levels of **5** and **6** Compared with **(1,2-b)-DSF-IF**, **(1,2-b)-IF**, and **2**

	E_{Ox} (V) ^f	E_{Red} ¹ (V) ^g	HOMO (eV) ^a	LUMO (eV) ^b	ΔE^{el} (eV) ^c	ΔE^{op} (eV) ^d	ΔE^{cal} (eV) ^e
5	1.33, 1.61 1.79, 2.03	–2.36	–5.61	–2.20	3.41	3.49	4.19
6	1.24, 1.55 1.84, 1.96	–2.52	–5.48	–2.05	3.43	3.53	4.16
(1,2-b)-IF	1.31, 2.02	–2.56	–5.62	–1.99	3.63	3.61	4.30
(1,2-b)-DSF-IF	1.43, 1.87	–2.25	–5.76	–2.17	3.59	3.51	4.18
2	1.44, 1.91	–2.73	–5.45	–1.03	4.42	3.93	–

^a From the onset oxidation potential. ^b From the onset reduction potential. ^c $\Delta E^{\text{el}} = |\text{HOMO} - \text{LUMO}|$ from redox data. ^d From the edge of the absorption spectrum (in CH₂Cl₂). ^e $\Delta E^{\text{cal}} = |\text{HOMO} - \text{LUMO}|$ using Gaussian 03 B3LYP/6-31G* calculation on simplified models of **5** and **6**. ^f In CH₂Cl₂. ^g In DMF.

5 and **6**, respectively. These values are closer to the reduction potential of **(1,2-b)-IF** (–2.56 V) than to that of **2** (–2.73 V). Therefore, it is rational to assign the first oxidation and reduction process of **5** and **6** to indenofluorene centered electron transfers. Theoretical calculations on simplified models of both isomers corroborate the electrochemical assignments pointing to the indenofluorenyl character of the HOMO and LUMO for **5** and **6** (cf. the Supporting Information). The lower first oxidation potential of **6** with respect to **5** is due to the different structure of the two indenofluorenyl moieties. With related 1,2-benzofluorene and 2,3-benzofluorene positional isomers, a similar negative shift

of the first oxidation potential has been reported.²¹ Contrary to the nonsubstituted **(1,2-*b*)-DSF-IF**,⁶ anodic oxidation of **5** and **6** does not lead to any electrodeposition process as anticipated by the introduction of the blocking *tert*-butyl substituents on the fluorenyl units.

Following the work of Jenekhe,²² we estimated the HOMO/LUMO levels (Table 2). Compared to **(1,2-*b*)-DSF-IF** the HOMO level of **5** appears to be slightly higher and the LUMO level slightly lower. It therefore appears that, although the fluorene moieties are not involved in the primary oxidation and reduction, the donor effect of their *tert*-butyl substituents is felt by the spiro-linked indenofluorenyl backbone. The HOMO and LUMO levels of **6** lie at -5.48 and -2.05 eV, respectively. The similar electrochemical band gap values for **5** (3.41 eV) and **6** (3.43 eV) are consistent with the measured optical band gaps and also qualitatively consistent with the theoretical values obtained with DFT calculations. The UV-vis absorption spectrum of **5** exhibits the five characteristic absorption bands of its central **(1,2-*b*)-IF** building block.^{6,14} The spectrum of **6** exhibits a main absorption band slightly hypsochromically shifted by 4 nm, with respect to **5**, in accordance with previous observations on the **(1,2-*b*)-IF** and **(2,1-*a*)-IF** core.¹⁶ The photoluminescence spectra of **5** and **6** revealed a very small Stokes shift (3/4 nm) that confirms that both structures are very rigid. Compounds **5** and **6** are highly fluorescent with quantum yields of ca. 70% (Table 3, Figure 4).

Table 3. Optical and Thermal Properties of **5** and **6**

	λ_{Abs} (nm) ^a	λ_{Exc} (nm) ^a	λ_{Em} (nm) ^a	ϕ (%) ^b	T_d (°C) ^c
5	308, 314, 330, 337, 339, 345	345	348, 369	70	350
6	323, 338, 341	341	345, 363, 381	75	320

^a In cyclohexane. ^b The relative quantum yield ϕ was measured using standard procedures with reference to quinine sulfate in 1 N H₂SO₄ ($\phi = 0.546$).¹⁴ ^c Decomposition temperature T_d is defined as the temperature at which 5% loss occurs during heating.²³

Thermogravimetric analysis (cf. the Supporting Information) confirmed the good thermal stability of **5** and **6** (T_d of

(21) Bordwell, F. G.; Cheng, J.-P.; Bausch, M. J. *J. Am. Chem. Soc.* **1988**, *110*, 2867–2872.

(22) Kulkarni, A. P.; Tonzola, C. J.; Babel, A.; Jenekhe, S. A. *Chem. Mater.* **2004**, *16*, 4559–4573.

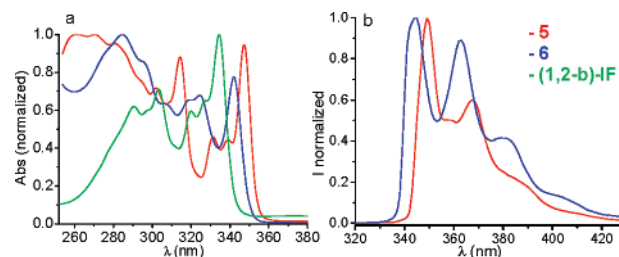


Figure 4. (a) UV-vis spectra of **5**, **6**, and **(1,2-*b*)-IF** in CH₂Cl₂. (b) Emission spectra of **5** and **6** in cyclohexane (10⁻⁶ M).

350 and 320 °C, respectively) as expected by the presence of the rigid, spiro-fused orthogonal linkages.^{23–25} Such behavior is highly important to improve the lifetime of blue OLED.

In conclusion, we have designed and synthesized two new dispiro isomer chromophores. These molecules are large band gap compounds with a high photoluminescence quantum yield in solution and are thermally stable. We demonstrated an efficient method for preparing these two positional isomers in different ratios depending on the reaction conditions. This method appears to be promising for preparing numerous compounds with the unique spirolinked **(2,1-*a*)-IF** backbone. Work is in progress on the elucidation of the mechanism of the cyclization reaction. An intimate understanding of the reaction is of great interest in preparing luminophores with well-defined geometry for future optoelectronic applications. These studies are underway in our laboratory.

Acknowledgment. We thank the C.R.M.P.O (Rennes), S. Sinbandhit for the 2D NMR study, the CINES (Montpellier) for computing time, Dr N. Audebrand for TGA, and S. Fryars for invaluable technical assistance.

Supporting Information Available: Experimental procedures and spectroscopic characterizations of new compounds. This material is available free of charge via the Internet at <http://pubs.acs.org>.

OL7026202

(23) Saragi, T. P. I.; Spehr, T.; Siebert, A.; Fuhrmann-Lieker, T.; Salbeck, J. *Chem. Rev.* **2007**, *107*, 1011–1065.

(24) Wong, K.-T.; Liao, Y.-L.; Lin, Y.-T.; Su, H.-C.; Wu, C.-C. *Org. Lett.* **2005**, *7*, 5131–5134.

(25) Kim, Y.-H.; Shin, D.-C.; Kim, S.-H.; Ko, C.-H.; Yu, H.-S.; Chae, Y.-S.; Kwon, S.-K. *Adv. Mater.* **2001**, *13*, 1690–1693.